Applied Thermal Engineering 29 (2009) 2194–2204

Contents lists available at ScienceDirect

Applied Thermal Engineering

journal homepage: www.elsevier.com/locate/apthermeng

Mixed Integer Nonlinear Programming model for the optimal design of fired heaters

Sergio Mussati [a,b,*], Juan I. Manassaldi [a], Sonia J. Benz [a], Nicolas J. Scenna [a,b]

[a] Universidad Tecnológica Nacional UTN-FRRo., Zeballos 1341, S2000BQA, Rosario, Argentina
[b] INGAR/CONICET, Instituto de Desarrollo y Diseño, Avellaneda 3657, 3000 Santa Fe, Argentina

ARTICLE INFO

Article history:
Received 19 January 2008
Accepted 3 November 2008
Available online 11 November 2008

Keywords:
Optimal fired heater design
General Algebraic Modelling System GAMS
MINLP models
Optimization model of heat transfer equipments

ABSTRACT

In this paper, a mathematical optimization model for the optimal design of industrial furnaces/fired heaters is presented. Precisely, a detailed Mixed Integer Nonlinear Programming (MINLP) model including operational and geometric constraints is developed to get an efficient furnace design. Discrete decisions connected with the geometric design such as number of tubes in convection and radiation sections, number of shield tubes, number of passes and number of tubes per pass are modelled by using integer variables. Continuous variables are used for process conditions (temperatures, flow-rates, pressure, velocities, pressure drops among others).

The mathematical model and the solution procedure are implemented in General Algebraic Modelling System (GAMS), Brooke [A. Brooke, D. Kendrick, A. Meeraus, A. A. GAMS – A User's Guide (Release 2.25), The Scientific Press, San Francisco, CA, 1992]. Based on a typical furnace configuration, several applications are successfully solved by applying the proposed MINLP model. In this paper, three case studies with increasing complexity are presented. In the first case study, the accuracy of results from the proposed model is compared satisfactorily with literature. In the second case study, the MINLP model is applied to optimize the fire heater's efficiency. Finally, the total annual cost of the fired heater is minimized in the Case Study III. Also, a sensitive analysis of the unitary cost of fuel and capital investment is investigated. The developed model is characterized by its robustness and flexibility.

1. Introduction

Furnaces are frequently used as hot utility systems of most processes plants and complex industrial units. Tubular furnaces are primarily used for heating all types of hydrocarbons and also hot oils and steam, becoming major consumers of energy in process plants. The design of the direct fired heater is inherently complex due to the complicated heat transfer situation given by convection and radiation mechanisms. Radiation is an important issue in furnaces because of its temperature; besides, gases at combustion-chambers temperatures lose more than 90% of their energy by radiation from the carbon dioxide, water vapour, and particulate matter. The optimization of fired heaters, boilers and/or furnaces is one of the most crucial tasks for increasing the efficiency of heat and power plants. As such equipments are highly energy demanding, even a minor efficiency improvement in its design can produce a significant decreasing of capital and operational costs. Indeed, to develop a model in order to solve the synthesis of complex processes, it is important to develop detailed and rigorous models for the fired heaters, boilers and/or furnaces.

There are several limitations on fired heater/furnace design since the efficiency, the maximum allowable absorption rate in the radiant section, the maximum allowable pressure drop of the process fluid in the heater, among others, strongly affect the optimal radiant tube system geometry (i.e., the number of tube, tube spacing, tube diameter, tube length, tube arrangement, radiant chamber size, etc.) and optimal combustion conditions (fuel type and costs, excess air rates, process fluid temperatures, etc.).

Wimpress [2] reported an iterative rating procedure for computing the performance of both the radiant and convection sections of fired heaters, given a typical design configuration. So, some aspects about the heater configuration, size and performance have to be imposed in advance to get the determined equation system to be solved over and over by modifying progressively the design variable values to adjust the heat transfer in each section to the required values. The Wimpress procedure proved to be a very efficient tool for rating the performance of the furnace according to a given design with a minimum of trial and error computation. That procedure is not suitable for optimization purposes, however.

Stehlík et al. [3] presented a simple mathematical model for fast simulation of various types of furnaces. The model consists of submodels for radiation chamber and convective sections including a sub-model of shield tubes for taking into account the connection

* Corresponding author. Address: INGAR/CONICET, Instituto de Desarrollo y Diseño, Avellaneda 3657, 3000 Santa Fe, Argentina. Tel.: +54 341 4480102/342 4534451; fax: +54 342 4553439.
E-mail address: mussati@ceride.gov.ar (S. Mussati).

1359-4311/$ - see front matter © 2008 Elsevier Ltd. All rights reserved.
doi:10.1016/j.applthermaleng.2008.11.001

Nomenclature

A_{cp} (m^2) cold plane area
A_{cp}^{shield} (m^2) cold plane area of shield tubes
A_{cp}^{wall} (m^2) cold plane area of wall tubes in firebox
A_R (m^2) refractory area
A_{rad} (m^2) radiant heat transfer area
A_{conv} (m^2) convection heat transfer area
MBL (m) mean beam length
c1, c2, c5 constant values of correlations
C_{cost} ($/yr) cost of convection section
c_{cost} ($/$m^2$) unitary cost of convection section
CRF ($year^{-1}$) capital recovery factor
d_C (m) distance between tube centers
D_O (m) outer tube diameter
D_{fb} (Pa) draft effect of the firebox
D_s (m) inner stack diameter
D_{stack} (Pa) draft effect of the stack
E_l (m) exposed length of the tube
e gas emissivity
ex_{air} (%) percent excess air
f correction factor
Ff fanning friction factor
FB_{cost} ($/yr) firebox cost
G (Kg/m^2 s) mass velocity at minimum cross-section
h_{Cc} (Watt/(m^2 K)) convective gas film coefficient
h_{Cr} (Watt/(m^2 K)) gas-radiation coefficient
h_{Cw} (Watt/(m^2 K)) wall-radiation coefficient
h_C (Watt/(m^2 K)) total apparent gas film coefficient
h_{Ci} (Watt/(m^2 K)) in tube film coefficient
h_c (J/mol) cross-over enthalpy of oil
h_i (J/mol) inlet enthalpy of oil
h_o (J/mol) outlet enthalpy of oil
H (m) height of firebox
H_s (m above shield tubes) stack height
k_l (m) unexposed length of the tube
L (m) furnace length
L_{equiv} (m) equivalent length of pipe
LMTD (K) logarithm means temperature difference from flue gas to fluid
MBL (m) mean Beam Length
M_{oil} (Kg/h) oil mass flow-rate
N_Passes total number of banks
OT (h/yr) plant Operating Time
O_{cost} ($/yr) operating cost
o_{cost} ($/J) unitary cost of fuel
Δp_b (Pa) pressure drop across the burners
Δp_f (Pa) pressure drop across horizontal tubes
Δp_l (Pa) various remaining pressure drop
p_h (Pa) velocity-head in the convection section
p_{hs} (Pa) velocity-head in the stack
P (KPa) partial pressure
Q_A (MWatt) heat absorbed by the oil
Q_n (MWatt) net heat-released from the fuel combustion
Q_l (MWatt) loss heat to the surroundings
Q_{rad} (MWatt) heat transfer rate absorbed in the radiant section
Q_{conv} (MWatt) heat transfer rate in the convection section
Q_{gr} (MWatt) heat content of gas leaving the radiant section
Q_{gs} (MWatt) heat content of gas leaving the convection section
R_{cost} ($/yr) cost of radiant section
r_{cost} ($/$m^2$) unitary cost of radiant section
T_a (K) outside air temperature
T_c (K) cross-over oil temperature
T_g (K) exit gas temperature
T_{fb} (K) average firebox temperature
T_i (K) inlet temperature of oil
T_o (K) outlet temperature of oil
T_s (K) inlet stack temperature
T_{gf} (K) average gas film temperature (convection section)
T_{gc} (K) average gas temperature (convection section)
T_{wc} (K) average tube wall temperature (convection section)
$Tube_l$ (m) tube length
T_w (K) average tube wall temperature
U (Watt/(m^2 K)) over-all transfer coefficient
V_S (m/s) velocity in stack
W (m) wide of firebox

Integer variables
Nt^{Rad} number of tubes on radiant section
Nt^{Conv} number of tubes on convection section
Nt^{Shield} number of tubes on shield section
$Nt^{wallside}$ number of wallside tubes
Nt^{ceil} number of ceiling tubes
Row_{Conv} number of rows on the convection section
Comp integer variable to force the number of shield tubes to be pair
Nt^{Bank} number of tubes per pass

Greek symbols
α absorptivity of a tube surface with a single row of tubes, dimensionless
η_{FH} fired heater efficiency, dimensionless
σ Stefan Boltzmann constant

between them. Some innovative procedures concerning combined heat transfer and model's possible applications were emphasized. That model proved itself to be a useful tool in a new methodology for furnaces integration into processes.

Jegla et al. [4] developed an efficient methodology for furnaces retrofit using optimization of both stack temperature and air preheating system. The method is based on process integration using *Pinch Analysis* to contribute to energy (fuel) saving. The proposed approach combines principles for getting an effective design from both processes and equipment. The method was exemplified and tested through a case study for a retrofit of a furnace in a hydrogenation refining petrol plant. Utilization of flue gas exhaust heat for air preheating together with a minor change in operating parameters resulted in approximately 20% reduction of annual plant energy costs.

Recently, Jegla [5] presented a procedure for the preliminary design of a tubular furnace considering mainly the design method of the radiant chamber. The conceptual radiant chamber design based on standard design methods (Lobo–Evans and Belokon's methods), was simplified in an effective manner to iteratively obtain basic design for a given furnace type including dimensions of radiant chamber. For selected values of design parameters, obtained data were connected with standard procedures for the design of the convection section and stack in order to obtain the whole vertical cylindrical furnace preliminary design. An objective function in terms of the total annual cost was introduced to search the optimum design.

A lot of effort and work have been put into the modelling and optimizing combustion-chambers, furnaces and fired heaters in the field of Computational Fluid Dynamics (CFD). CFD is being used

widely all over the world in many different engineering applications, where the knowledge of fluid flow, temperature, pressure, velocity, turbulence, and compositions profiles and behaviors is critical in the design and optimization of several equipments. Moreover numerous variations of the detailed engineering of the involved apparatuses can be simulated before realization.

Marek Sarlej et al. [6] applied computational fluid dynamics (CFD) technique in experimental burner design. The aim of the work consisted in finding an optimal geometrical arrangement of the secondary fuel nozzles with respect to the global NOx production. The possibility of utilization of CFD in terms of finding optimum arrangement of secondary fuel nozzles of an experimental burner was demonstrated. A number of alternatives of secondary nozzle arrangement were investigated with respect to NOx production. Finally, an alternative corresponding to minimum NOx production was identified.

Miltner et al. [7] showed that the joint application of process simulation and computational fluid dynamics (CFD) is a helpful tool for the design and optimization of complex and innovative concepts in chemical engineering practice. The application of these tools to the biomass-fired combustion chamber allowed the optimization of operation parameters such as the flue gas recirculation rate and excess air supply. The major goals comprise the maximization of the thermal efficiency and the reduction of gaseous and particulate matter emissions.

Other recent applications of CFD in the process industry, concerning the design, scale-up, revamp, troubleshooting, and operation optimization of process equipments as heat exchangers, furnaces, reactors, distillation columns, toxic and flammable gas detection systems can be found in [8].

However, by considering the state of the art for rigorous and complex model optimization using mathematical programming, CFD is not suitable to simultaneously optimize discrete (configuration) and continuous decisions because the combinatorial nature of the problem. Using CFD models, optimized process designs are achieved by simulating different alternative configurations and then, the best design is obtained by comparing the results from simulations. For some cases, the application of CFD can lead to large computing time as well as memory requirements.

The goal of this paper is to develop a mathematical model to simultaneously optimize the discrete and continuous decisions. To do this, natural approach is the use of Mixed Integer Nonlinear Programming (MINLP) and/or Generalized Disjunctive Programming (GDP) techniques, which make difficult the modelling task using CFD technique.

Precisely, a detailed Mixed Integer Nonlinear Programming (MINLP) model including operating (continuous) and geometrical constraints is formulated to get an efficient fired heater design, considering at once the radiant chamber, the convection section and stack.

Discrete decisions connected with the geometric design such as number of tubes in convection and radiation sections, number of shield tubes, number of tubes per pass, are modelled by using integer variables. Continuous variables are used for process conditions and sizes (temperatures, flow-rates, pressure, velocities, pressure drops, and dimensions, among others).

The developed MINLP model and solution procedure are implemented in GAMS.

The paper is outlined as follows: Section 2 briefly describes different fired heater configurations indicating the configuration selected to be studied in this paper. Section 3 introduces the problem formulation. Section 4 summarizes the assumptions, the mathematical model and the resolution procedure. Section 5 presents applications of the developed MINLP model and results analysis. Finally, Section 6 presents the conclusions and future work.

2. Description of the furnace

Tubular furnaces (or fired heaters) are large, complex items used in chemical, petrochemical, and refinery process. Furnace designs vary as to its function, heating duty, type of fuel and method of introducing combustion air. Different typical furnace configurations for petroleum applications are shown in Fig. 1. The preferred design of furnaces is mostly of the radiation–convection type, since it uses the flue gas heat more effectively getting higher thermal efficiency and lower fuel consumption (lower operating costs) than the stand alone convection or radiation types. Some types of process fired heaters presented in Fig. 1 are: (a) radiant, shield, and convection sections of a box-type heater; (b) heater with a split convection section for preheating before and soaking after the radiant section – Lobo and Evans [9]; (c) vertical radiant tubes in a cylindrical shell and, (d) Two radiant chambers with a common convection section.

As can be seen in Fig. 1, furnaces have some common features, however. The main parts of a furnace are the radiation chamber, convection section, burners, tubes, and stack.

The heat input is provided by burning fuel, usually oil or gas, in the combustion chamber. Fuel flows into the burner and is burnt with air provided from an air blower.

The combustion takes place in a firebox without flame impingement on tubes or refractory walls. There can be more than one burner in a particular furnace which can be arranged in cells which heat a particular set of tubes. Burners can also be floor mounted, wall mounted or roof mounted depending on design. The flames heat up the tubes, which in turn heat the fluid inside the radiant section.

In the firebox, the heat is transferred mainly by radiation to tubes around the fire in the chamber. In this section, tubes can be vertical (Fig. 1c) or horizontal (Fig. 1a, b, and d), placed along the refractory wall, in the middle or arranged in cells. The tubes on this section, which are reddish brown from corrosion, are carbon steel tubes and run the height of the radiant section. The tubes are a distance away from the insulation so radiation can be reflected to the back of the tubes to maintain a uniform tube wall temperature.

The heating fluid passes through the tubes and is thus heated to the desired temperature. The gases from the combustion are known as flue gas. After the flue gas leaves the firebox, most furnace designs include a convection section which is located above the radiant section where more heat is recovered before venting to the atmosphere through the flue gas stack.

In the convection section the tubes are finned to increase heat transfer. The first two tube rows in the bottom of the convection section and at the top of the radiant section is an area of bare tubes (without fins) and are known as the shield section, so named because they are still exposed to plenty of radiation from the firebox and they also act to shield the convection section tubes, which are normally of less resistant material from the high temperatures in the firebox.

The area of the radiant section just before flue gas enters the shield section and into the convection section called the bridge zone. Cross-over is the term used to describe the tube that connects from the convection section outlet to the radiant section inlet. The cross-over piping is normally located outside so that the temperature can be monitored and the efficiency of the convection section can be calculated.

Insulation is an important part of the furnace because it prevents excessive heat loss. Refractory materials such as firebrick, castable refractories and ceramic fibre, are used for insulation.

In fire heater schemes presented in Fig. 1, some of the convection tubes are used for preheat and the remainder to maintain the process fluid at a suitable reaction temperature that was attained in the radiant tubes. The double ascendant burnt type fire

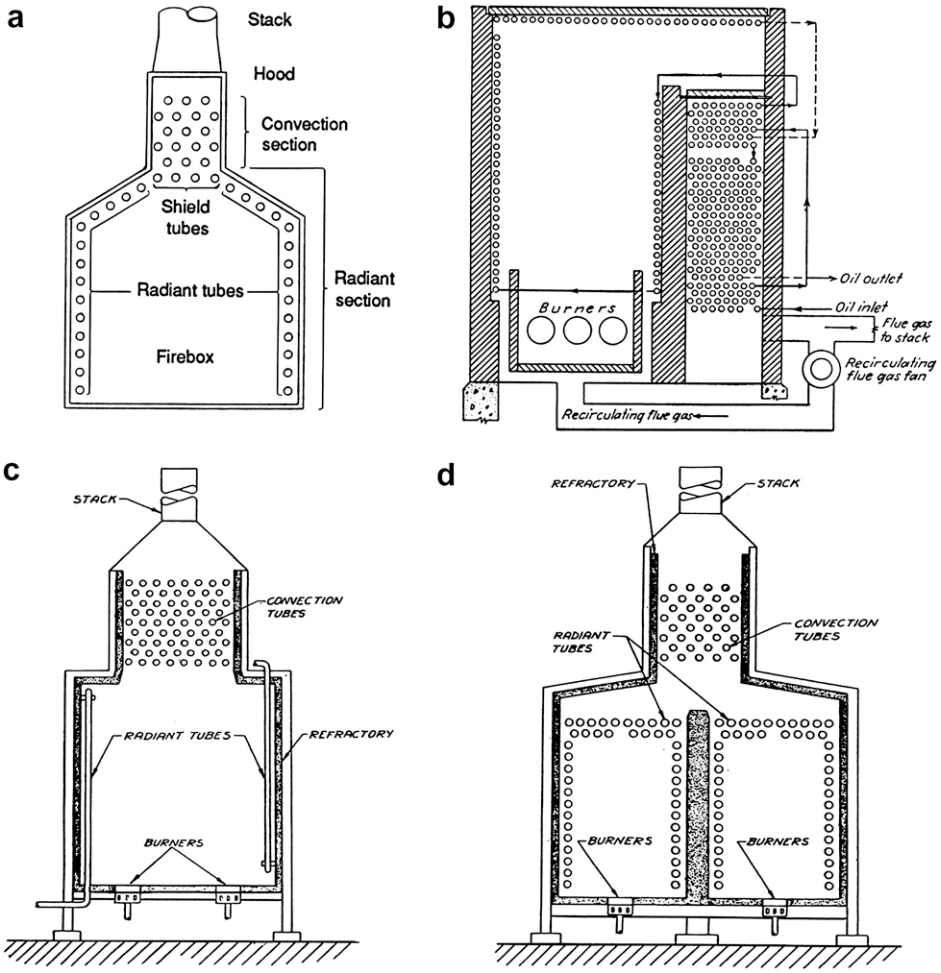

Fig. 1. Different fire heater configurations.

heater (Fig. 1a) allows a medium/big capacity and high well controlled heat fluxes with a central burner and short stack. In the more complex flow pattern of Fig. 1, the proportions of heat transferred in the radiant and convection zones can be regulated by recirculation of hot flue gases into the radiant zone, as sketched on Fig. 1b. Such an operation is desirable in thermal cracking of hydrocarbons, for instance, to maintain a proper temperature profile; a negative gradient may cause condensation of polymeric products that make coke on the tubes. The circular fire heater with vertical tubes (Fig. 1c) has generally big capacity and high costs with excellent radiant distribution and very short stack. On the other hand, multiple radiant chambers are preferred as process fluid goes first through the convection section and usually leaves the radiant tubes at the top, particularly when vaporization occurs in them (Fig. 1d). Some of the convection zone also may be used for steam generation or superheating or for other heat recovery services in the plant.

The configuration shown in Fig. 1a will be studied in detail in this paper.

3. Problem formulation

The problem can be stated as follows: Given the type of oil to be heated, the inlet/outlet pressure, temperature conditions and the configuration of a fired heater (cabin furnace type), the goal is to determine the optimal geometric design and compute the optimal operating conditions in order to satisfy the required heating duty by maximizing the process efficiency and/or minimizing the total annual cost, depending on which objective function is used to optimize the process.

Precisely, dimensions on radiant chamber and convection sections, number and array of tubes in radiation and convection sections, number of shield tubes, average heat flux, net absorbed heat, heat transfer area in both heating sections as well as fuel consumption, are simultaneously optimized.

4. MINLP mathematical model for the cabin furnace

In this section, the adopted hypothesis and the mathematical model for the fired heater shown in Fig. 1a are presented.

4.1. Assumptions

- Flue gas complete mixture in the firebox assuring no longitudinal and transverse temperature gradients.
- The radiant section is "well mixed". The average gas temperature equals the temperature of the gas leaving the radiant section.
- Radiant arrangement is assumed as box.
- Tubes are placed horizontally and symmetrically along the refractory wall.

For most applications, these assumptions are widely accepted and usually employed for modelling purposes. So, the following mathematical model can be formulated.

4.2. Mathematical model

A given oil flow-rate (M_{oil}) is heated in a furnace from an inlet temperature (T_i) to a desired outlet temperature (T_o). In Fig. 2, a schematic representation of the heating transfer process in the radiant and convection sections is presented. The oil passes through absorbing the net available gas combustion heat. The total heat transferred from the radiant and convection sections to the oil (Q_A) is computed by Eq. (1).

$$Q_A = M_{oil}(h_{out} - h_{in}) = Q_{rad} + Q_{conv} \quad (1)$$

where h refers to oil enthalpy, with h = h(T). Q_{rad} and Q_{conv} refer to the heat transfer rate absorbed in the radiant and convection sections, respectively.

Net heat-released from gas combustion (Q_n) is computed considering the fire heater efficiency (η_{FH}) by Eq. (2).

$$\eta_{FH} = \frac{Q_A}{Q_n} \quad (2)$$

Also, the net released heat must satisfy the whole energy balance for the radiant and convection section together, including the loss heat rate to the stack and the surroundings, as expressed in the following equation:

$$Q_n = Q_{rad} + Q_{conv} + Q_l + Q_{gs} \quad (3)$$

where Q_l and Q_{gs} refer to the loss heat to the surroundings and the heat content of gas leaving the convection section, respectively.

4.2.1. Radiant section

Heat transfer in the radiant zone of a fired heater occurs largely by radiation from the flue gas (90% or so) but also significantly by convection. The combined effect is represented by Eq. (4),

$$\frac{Q_{rad}}{\alpha A_{cp} F} = \sigma(T_{fb}^4 - T_w^4) + 7(T_{fb} - T_w) \quad (4)$$

where T_{fb} and T_w refer to the average firebox temperature and average tube wall temperature, respectively. σ refers to the Stefan Boltzmann constant.

The absorptivity (α) depends on the tube spacing (d_C) and the outer diameter tube (D_O).

$$\alpha = c_1\left(\frac{d_C}{D_O}\right)^2 + c_2\left(\frac{d_C}{D_O}\right) + c_3 \quad (5)$$

where c_1, c_2, c_3 are constant values.

The cold plane area (A_{cp}) is calculated as the product of the number of tubes by their lengths and by the center-to-center spacing. Factor (αA_{cp}) is equal to the area of an ideal black plane that has the same absorptivity as the tube bank, and is named the equivalent cold plane area. The exchange factor (F) depends on the emissivity of the gas (e) and the ratio of refractory area (A_R) to the equivalent cold plane area (αA_{cp}).

$$F = c_1\log(e) + c_2\left(\frac{A_R}{\alpha A_{cp}}\right) + c_3\left(e\frac{A_R}{\alpha A_{cp}}\right) + c_4\exp(e) + c_5\left(e\frac{A_R}{\alpha A_{cp}}\right)^{1.5} + c_6 \quad (6)$$

$$A_R = A - \alpha_{cp} \quad (7)$$

where A is the area of the inside walls, roofs, and floor that are covered by refractory.

$$A = 2WH + 2L(W + H) \quad (8)$$

W, H and L refer to width, height and length of the firebox, respectively.

Equivalent cold planes for shield tubes (A_{cp}^{shield}) and wall tubes (A_{cp}^{wall}) in the fired box are respectively computed by Eqs. (9) and (10).

$$A_{cp}^{shield} = E_l \times Nt^{Shield} \times \frac{d_C}{12} \quad (9)$$

$$A_{cp}^{wall} = E_l \times (Nt^{Rad} - Nt^{Shield}) \times \frac{d_C}{12} \quad (10)$$

where Nt^{Shield} and Nt^{Rad} refer to the number of tubes in shield and radiation sections, respectively.

The exposed length of the tube (E_l) and the inside length of the furnace (L) are shorter than the tube length ($tube_l$).

$$E_l = L = tube_l - k_l \quad (11)$$

where k_l refers to the unexposed length of tube.

The total equivalent cold planes results from,

$$\alpha A_{cp} = A_{cp}^{shield} + \alpha A_{cp}^{wall} \quad (12)$$

The emissivity (e) can be correlated as a function of the gas average temperature equivalent to fire box temperature (T_{fb}) and PL factor.

$$e = c_1 T_{fb} + c_2 PL + c_3(PL)^2 + c_4 \quad (13)$$

PL factor is computed as follows:

$$PL = P_{(CO_2+H_2O)}MBL \quad (14)$$

$$MBL = \frac{2}{3}(L \times W \times H)^{\frac{1}{3}} \quad (15)$$

$$P_{CO_2+H_2O} = c_1(ex_{air})^3 + c_2(ex_{air})^2 + c_3(ex_{air}) + c_4 \quad (16)$$

where $P_{CO_2+H_2O}$ and MBL refer to the partial pressure of the carbon dioxide and water and Mean Beam Length, respectively (Lobo and Evans [9]).

The radiant section heat balance must be also satisfied according to:

$$Q_{rad} = Q_n - Q_l - Q_{gr} \quad (17)$$

In analogy way Eq. (4) is got, the above equation (Eq. (17)) can be transformed into the next equation.

$$\frac{Q_{rad}}{\alpha A_{cp} F} = \left[1 - \frac{Q_l}{Q_n} - \frac{Q_{gr}}{Q_n}\right]\frac{Q_n}{\alpha A_{cp} F} \quad (18)$$

The heat loss (Q_l) is usually considered in the range from 1% to 3% of the net heat-release (Q_n). Here we adopted 2%:

$$\frac{Q_l}{Q_n} = 0.02 \quad (19)$$

The fraction of net heat-release retained in the flue gas leaving the radiant section is primarily a function of temperature and excess air, for all common liquid and gaseous fuels.

$$\frac{Q_{gr}}{Q_n} = c_1 T_g^{c_2}\left(1 + \frac{ex_{air}}{100}\right)^{c_3} \quad (20)$$

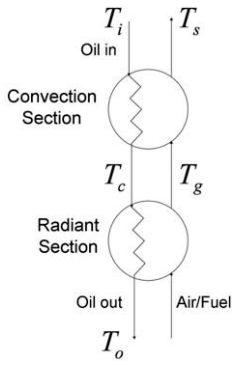

Fig. 2. A schematic representation of the heating transfer process in the radiant and convection sections.

Experience has shown that the average gas temperature (T_{fb}) is very close to that of the exit gas (T_g) for box fired heater types here analyzed.

$$T_g = T_{fb}$$

The tube wall temperature (T_w) depends on many factors such as the temperature of the fluid inside, the inner tube transfer coefficient, among others. It is usually accurate enough to add an adequate Δt-value to the average fluid temperature, which is computed as the arithmetic mean of the radiant section inlet and outlet oil temperature, T_c and T_o, respectively. The radiant section inlet oil temperature (T_c) is named from here cross-temperature.

So, the tube wall temperature (T_w) can be computed by:

$$T_w = \frac{T_o + T_c}{2} + \Delta t \tag{21}$$

The cross-over temperature from convection to radiant section is calculated from process fluid enthalpy according to the following equations.

$$h_c = h_o - \frac{Q_{rad}}{M_{oil}} \tag{22}$$

$$h_c = c_1(T_c)^2 + c_2(T_c) + c_3 \tag{23}$$

4.2.2. Convection section

The furnace design requires the computation of the heat transfer areas in each furnace section. In particular, the heat transfer area for the convection section (A_{conv}) is computed as follows:

$$Q_{conv} = Q_A - Q_{rad} \tag{24}$$

$$A_{conv} = \frac{Q_{conv}}{U \times LMTD} \tag{25}$$

where LMTD refers to the logarithm mean temperature difference which is defined as follows:

$$LMTD = \frac{(T_g - T_c) - (T_s - T_i)}{\ln\left(\frac{T_g - T_c}{T_s - T_i}\right)} \tag{26}$$

The over-all transfer coefficient in the convection section (U) is computed by:

$$U = \frac{h_C(h_{Ci})}{h_C + h_{Ci}} \tag{27}$$

Coefficient (U) is based on the total apparent gas film coefficient (h_C) that is determined by the following equation, from the individual coefficients and a correction factor f.

$$h_C = (1 + f)(h_{Cc} + h_{Cr}) \tag{28}$$

The following constraint computes the correction factor (f) which depends on the relative wall and tube areas in the convection section:

$$f = \frac{h_{Cw}}{h_{Cc} + h_{Cr} + h_{Cw}}\left(\frac{A_{Cw}}{A_{Ct}}\right) \tag{29}$$

The individual transfer coefficients for computing the total apparent coefficient in the convective section are summarized below, according to each transfer mechanism.

Convective gas film coefficient:

$$h_{Cc} = c_1 T_{gf} + c_2 G + c_3 G^2 + c_4 T_{gf} G + c_5$$
$$\text{where } T_{gf} = \frac{(T_i + T_c)}{2} + \frac{LMTD}{2} \tag{30}$$

Flue gas-radiation coefficient:

$$h_{Cr} = f(T_{gc}, T_{wc}) = c_1 T_{wc}^{0.05} + c_2 T_{gc}^{0.05} + c_3 \log\left(\frac{T_{gc} T_{wc}}{c_4}\right) + c_5$$
$$\text{where } T_{gc} = \frac{(T_i + T_c)}{2} + LMTD \tag{31}$$

Refractory walls radiation coefficient:

$$h_{Cw} = f(T_{wc}) = c_1 T_{wc}^3 + c_2 T_{wc}^2 + c_3 T_{wc} + c_4$$
$$\text{where } T_{wc} = \frac{(T_i + T_c)}{2} + \Delta t \tag{32}$$

In Eq. (30), the flue gas rate (G) is at the minimum cross-section in the convection section. The average gas film temperature (T_{gf}) is defined as the average in tube fluid temperature plus one-half the log mean temperature difference from flue gas to fluid.

In Eq. (31), the average gas temperature (T_{gc}) is defined as the average in tube fluid temperature plus the log mean temperature difference from the flue gas to fluid. The average tube wall temperature (T_{wc}) may be taken as average fluid temperature plus an adequate Δt (Eq. (32)).

4.2.3. Whole radiant and convection section

Eq. (3) can also be written as:

$$\frac{Q_n}{Q_n} = \frac{Q_{rad} + Q_{conv}}{Q_n} + \frac{Q_l}{Q_n} + \frac{Q_{gs}}{Q_n}$$

Taking into account the Eq. (19), that can be equivalently expressed as,

$$\eta_{FH} = 1 - \frac{Q_l}{Q_n} - \frac{Q_{gs}}{Q_n} \tag{33}$$

The gas heat content entering the stack depends on gas temperature at that point (T_s) and the air excess (ex_{air}) used in the gas combustion according to a given functionality,

$$\frac{Q_{gs}}{Q_n} = c_1 T_s^{c_2}\left(1 + \frac{ex_{air}}{100}\right)^{c_3} \tag{34}$$

From Eqs. (33) and (34), the fired box efficiency (η_{FH}), which depends on the gas temperature at the inlet stack and the used air excess, is computed according to the following equation:

$$\eta_{FH} = f(T_s, ex_{air}) = 0.98 - c_1 T_s^{c_2}\left(1 + \frac{ex_{air}}{100}\right)^{c_3} \tag{35}$$

4.2.4. Additional design restrictions for convection and radiant sections

A set of additional design restrictions are included in the present mathematical model to approach the sought solution according to actual furnace design hints.

The two following dimension constraints are added in order to ensure the validity of the mean beam length equation (Eq. (14)),

$$1.8 \leqslant \frac{L}{W} \leqslant 3 \tag{36}$$

$$1 \leqslant \frac{H}{W} \leqslant 1,5 \tag{37}$$

Besides, Eq. (37) implies an approximately square cross-section for box fired heaters, to assure only one transfer regime into the radiant section.

In Fig. 3 it is shown a furnace scheme indicating the relationships among tube configurations inside it and the nomenclature. In the convection section, the tube size, pass arrangement, number of tubes a row and number of rows are selected according to the

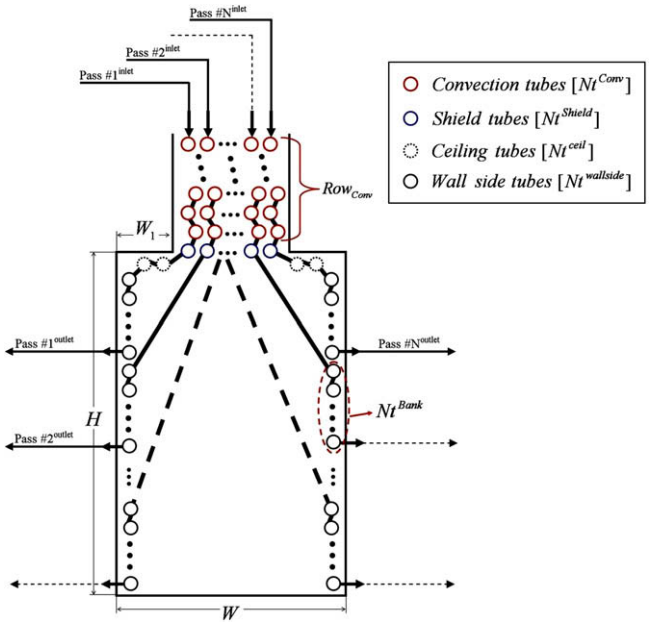

Fig. 3. Furnace scheme.

calculated total convection surface and the specific pressure drop limitations. In the radiant section, the heat absorbing surface is usually achieved by a number of parallel cylindrical tubes in front of a refractory wall. The number of shield tubes allows computing the pairs of tube banks arranged in front of both refractory walls.

It is known that the tube net length (E_l) and the tube cross-section (s) must satisfy Eq. (9), (10), (18), (38) and (44) among others, both dimensions limit the tube available transfer surface and therefore, the required number of tubes to satisfy the energy balance equations.

$$L = E_l = tube_l - k_l \tag{38}$$

$$s = \pi D_O \tag{39}$$

$$Nt^{Conv} = \frac{A_{conv}}{sE_l} \tag{40}$$

$$Row_{Conv} = \frac{Nt^{Conv}}{Nt^{Shield}} \tag{41}$$

The following equations are used to compute the number of passes in radiant chamber (see Fig. 3).

The total number of tubes in radiant section (Nt^{Rad}) is computed by summation of the number of wallside tubes ($Nt^{wallside}$), ceiling tubes (Nt^{ceil}) and shield tubes (Nt^{Shield})

$$Nt^{Rad} = Nt^{wallside} + Nt^{ceil} + Nt^{Shield} \tag{42}$$

$Nt^{wallside}$ and Nt^{ceil} are related with the dimensions of the firebox (H and W1) by the following constraints:

$$\left(\frac{Nt^{wallside}}{2} - 1\right) * d_C/12 + kk1 = H \tag{42a}$$

$$\left(\frac{Nt^{ceil}}{2} - 1\right) * d_C/12 + kk2 \leqslant W_1 \tag{42b}$$

where kk1 and kk2 are constants which take into account tube diameter, tube arrangement and distance to refractory, among others. W1 refers to the length required to accommodate the number of tubes $Nt^{ceil}/2$ (see Fig. 3).

The number of tubes per bank (Nt^{Bank}) is computed as follows:

$$Nt^{Bank} = \frac{(Nt^{ceil} + Nt^{Shield})}{Nt^{Shield}} \tag{42c}$$

Finally, the total number of banks (N_Passes) in radiant chamber is computed as follows (see Fig. 3):

$$N\_Passes = Pass\#1^{outlet} + Pass\#2^{outlet} + \ldots + Pass\#3^{outlet} = Nt^{Shield}.$$

As the tube configuration in the radiation section depends on the shield tubes configuration, it is necessary to include an additional integer variable (Comp) that forces the number of shield tubes be pair for assuring a symmetric distribution of radiant tubes banks at each side of the fired box, as can be observed in the Fig. 3.

$$Comp = \frac{Nt^{Shield}}{2} \tag{43}$$

Besides, in order to preserve the construction materials of the fired box, a maximum value for radiation flux (Flux) is considered,

$$Flux = \frac{Q_{rad}}{sE_l Nt^{Rrad}} < 12000 \frac{Btu}{hft^2} \tag{44}$$

Lower and upper bounds for velocity stack (V_s), mass velocity (G) and box size are included in order to restrict the variation range of some optimization variables – Couper et al. [10].

$$28.5 \leqslant V_s \leqslant 31 \tag{45}$$

$$0.3 \leqslant G \leqslant 0.4 \tag{46}$$

$$3.5 < \frac{(L \times W \times H)}{sE_l Nt^{Rad}} < 4.5 \tag{47}$$

Constraint (47) is based on practical heuristics; a rough guide to box size is about 4 ft^3/ft^2 of radiant transfer surface for having enough space to avoid flame impingement on the tubes.

The fluid pressure drop of heated fluid Δp is computed by the following constraint:

$$\Delta p = \frac{0.00517}{d_C} G^2 V Ff \quad L_{equiv}$$

where d_C, G, V and Ff refer respectively to tube inside diameter, mass velocity of fluid, mean specific volume correction and fanning friction factor. L_{equiv} is the equivalent length of pipe.

4.2.5. Stack design

In a natural-draft heater, the stack must create enough draft to overcome frictional drop through burners, the convection section, the damper, and the stack.

$$D_{stack} = \Delta p_b - D_{fb} + \Delta p_f + \Delta p_l \tag{48}$$

D_{stack} and D_{fb} refer to the draft effect of the stack and fire heater, respectively. Δp_f refers to the pressure drop across horizontal tubes.

Pressure drop across burners (Δp_b) is usually set by the burner manufacturer. The pressure drop across horizontal tubes in the convection section is computed by:

$$\Delta p_f = Row_{Conv} \frac{p_h}{2} \tag{49}$$

The velocity-head measured in inches of water is given by the following equations.

$$p_h = 0.003 \frac{G_2}{\rho_g} \tag{50}$$

D_{fb} and D_{stack} are computed respectively by,

$$D_{fb} = (c_1 T_g + c_2 T_a + c_3 \log(T_g) + c_4)(H - c_5) \tag{51}$$

$$D_{stack} = (c_1 (T_s - T_x) + c_2 T_a + c_3 \log(T_s - T_x) + c_4) H_s \tag{52}$$

where T_x is a constant fixed at 311 K (typical value).

The various remaining losses corresponding to the stack entrance, damper, stack friction and exit can be computed in terms of velocity-head in the stack and considered in the model through the following equation:

$$\Delta p_l = \left(3 + \frac{H_s}{50 D_s}\right) p_{hs} \quad (53)$$

4.2.6. Cost function

The objective function is built from costs considerations. The following equations are used to compute the capital investment:

$$R_{cost} = r_{cost} A_{rad} CRF \quad (54)$$

where R_{cost}, r_{cost} and A_{rad} refer to the cost of radiant coil, unitary cost and radiant heat transfer area, respectively. CRF refers to the capital recovery factor.

In the same way, the cost of convection coil (C_{cost}) is computed by the following equation;

$$C_{cost} = c_{cost} A_{conv} CRF \quad (55)$$

where C_{cost}, c_{cost} and A_{conv} refer to the cost of convection coil, unitary cost and convection heat transfer area, respectively.

The firebox cost (FB_{cost}) is computed by:

$$FB_{cost} = [k_1 + k_2 (A_{rad} + A_{conv})] CRF \quad (56)$$

where k_1 and k_2 are given values and they depend on the type of refractory, coil materials, insulation width, among others.

The operating cost, which only includes the fuel consumption and operating time, is computed by the following equation:

$$O_{cost} = o_{cost} Q_n OT \quad (57)$$

where o_{cost} is the unitary fuel cost and OT refers to the plant operating time.

$$T_{cost} = R_{cost} + C_{cost} + O_{cost} \quad (58)$$

The optimization mathematical model involves 123 variables (8 integer variables) and 110 constraints. The model is implemented in General Algebraic Modelling System GAMS. Standard Branch and Bound (SBB), Brooke [1], is used as solver for the resulting MINLP model. It is based on a combination of the Standard Branch and Bound method known from Mixed Integer Linear Programming and some of the standard NLP solvers already supported by GAMS.

5. Applications of the developed MINLP model

In this section, the proposed model validation with the literature, optimization results, and numerical and computational performance are presented through three case studies. The parameter data set listed in Table 1 was assumed for all examples.

All examples are solved using a 800 MHz Pentium IV processor and 2 GB RAM.

5.1. Case Study I

In this example, model outputs are compared with data from literature to test and validate the proposed model.

Table 1
Assumed parameters for all applications.

Parameter	Value
Flue gas rate (Kg/MJ)	4.342e−01
d_C (m)	0.2032
D_O (m)	0.1143
M_{oil} (Kg/s)	44.98124
T_i (K)	466.483
T_o (K)	630.37
Q_A (MWatts)	21.9715
ex_{air} (%)	25
T_a (K)	310.92
OT (h/yr)	8000

A rigorous model validation should be conducted jointly with heater manufacturers and/or petrochemical industries because numerous and complete dataset of real designs can be provided by them. Moreover, this dataset could be efficiently used to adjust the model parameters in order to improve the accuracy of the model if this is necessary. Least squares and bayesian methods, minimization of absolute deviations as well as nonparametric regression are widely used for parameter adjustment.

Because of real and complete designs provided by manufacturers (or petrochemical industries) are not available in the open literature to validate the proposed model, design data reported by Wimpress [2] are considered for comparison purposes since a complete solution of the furnace design was provided. However, an iterative solution procedure based on simulation runs had been applied instead of optimization techniques. Consequently, the values reported by Wimpress [2] are not optimal. Therefore, various optimization variables in the proposed MINLP model are fixed at the same values as in [2] for recreating the Wimpress case study, as listed in the second column of Table 2. Thus, the proposed mathematical model is here used more as a "simulator" than an optimizer.

In Table 3, the resulting values for the main practical interest variables of the fired heater according to the Wimpress design and the here proposed MINLP model are reported in the second and third columns, respectively. This last solution is hereafter named MINLP Design I.

As is shown in Table 3, the obtained values by the MINLP model are very similar to those reported by Wimpress [2]. As the MINLP type formulation here proposed is very complex since it integrates a high number of variables and equations, complex nonlinear correlations involving process variables as well as a detailed description of heat transfer phenomena, it can be concluded that the obtained solution agree satisfactorily with the design reported in Wimpress [2].

5.2. Case Study II

Here, an optimization problem is solved by "relaxing" the variable values that were fixed for Case Study I, specifically those listed in Table 2, which are now decision variables. The goal is to minimize the total heat transfer area and the refractory material area. The detailed solution is reported in Table 4, which is hereafter named MINLP-Design II. In addition, the optimal values obtained for the MINLP-Design II are compared with the values corresponding to the MINLP-Design I. Table 4 shows that the fired heater design is largely improved when both the total heat transfer area and the refractory material area are minimized. In fact, the MINLP-Design II involves fewer tubes (Nt^{Rad}, Nt^{Conv} and Row_{Conv}) than for MINLP-Design I. The fired heater dimensions (height and width) are also smaller, though the tube length is slightly longer. Besides, the total investment for MILNP-Design II is lower than for MINLP-Design I.

On the other hand, the stack height, the firebox size and the tube length of the radiant/convection sections for MINLP-Design II are larger than for MINLP-Design I.

Table 2
Fixed values for Case Study I (optimization variables in Case Study II).

Fixed values	Wimpress design	MINLP Design I
Nt^{Rad}	96	96
Nt^{Conv}	108	108
Nt^{Shield}	6	6
Row_{Conv}	18	18
W (m)	6.096	6.096
H (m)	7.62	7.62
$Tube_l$ (m)	12.192	12.192

Table 3
Comparison of solution between Wimpresśdesign and the proposed MINLP model.

Variable	Wimpresśs Design	MINLP Design I
Total tubing area (m^2)	893.0286	893.1023
η_{FH}	0.776	0.774
A (m^2)	415.276	414.8120
A_{rad} (m^2)	405.0572	404.5227
A_{conv} (m^2)	455.2248	455.0881
T_{fb} (K)	1149.8166	1151.4166
Flux (Watt/m^2)	37,381.9	36,913.5827
Q_{rad} (MWatt)	15.1224	14.9322
Q_{conv} (MWatt)	6.857	7.039
T_s (K)	699.8166	699.662
H_s (m above shield tubes)	19.812	19.927
R_{cost} ($/yr)	133,416	133,240
C_{cost} ($/yr)	88,200	88,173.51
F_{cost} ($/yr)	92,340	92,274.982
O_{cost} ($/yr)	1,545,773.196	1,549,100
TAC ($/yr)	1,859,729.196	1,862,800

5.3. Case Study III

An optimization problem aiming at the minimization of the Total Annual Cost (TAC), which includes investments and operating costs, is solved. Specifically, the investment cost calculation considers the heat transfer areas of the radiant and convection sections, as well as the firebox cost that depends on refractory material type and insulation thickness, among others. Fuel consumption is considered for the operating cost calculation.

The optimal economic design is reported in the second column of Table 5, which is hereafter named MINLP-Design III. In addition, it is compared against the optimal MINLP-Design II (third column of Table 5).

As can be seen, the cost related to the radiation zone (R_{cost}), the operating cost (O_{cost}) and the total annual cost (TAC) for MINLP-Design III are lower than for MINLP-Design II. The investment cost (C_{cost}) and firebox cost (F_{cost}) for Design III are higher, however. Regarding design characteristics, the number of tubes in the convection section (Nt^{conv}) and the transfer area are greater for MINLP-Design III; moreover, the convection tubes are placed in a greater number of rows (Row_{Conv}). On the other hand, for the radiation section, equal number of shield tubes (Nt^{Shield}) and equal number of tubes per pass (Nt^{Bank}) (4 and 18, respectively) are obtained for both MINLP-Design III and MINLP-Design II. The tube length for Design III is shorter than for Design II. Therefore, the heat transfer areas in the radiant section for Design III are lower. However, the total area results bigger, the upper bound on the heat flux is reached and the stack temperature (T_s) is about 30 K lower than for Design II.

As result of the above comparison, it is evident that the optimal economic MINLP-Design III renders a higher efficiency and a lower total annual cost.

5.4. Sensitive analysis. Performance of model and solver

A sensitive analysis of the unitary fuel cost and capital investment on the optimal design is also investigated. The fuel unitary cost and capital investment (heat transfer area unitary cost) were varied from −30% to 30% and were compared to the values used in the Case Study III.

From the obtained results, it is concluded that the design depends on the cost ratio. For example, the higher firebox cost, the shorter firebox dimensions. In this case, the total annual cost is increased in 1,867,500 (2.066% more expensive than Case Study III).

On the contrary, the lower firebox cost, the bigger firebox dimensions. In this case the total annual cost is decreased in 1,792,000 $/yr (2.1038/more cheap than Case Study III).

All in all, a slight variation on in the optimal design of the fired heater is observed when the fuel unitary cost was varied.

The robustness and flexibility of the model as well as the SBB algorithm have been examined by solving many examples which were conducted by varying the parameters values (inlet/outlet temperatures, heating duty). For all cases, optimal solutions were achieved without computational difficulties. However, due to space limitations the obtained results are not here reported.

In most cases, the chemical processes modelling as well as detailed and rigorous equipment models involve at least one (or more) nonconvex constraints which may lead to local optimal solutions or convergence problems. The proposed model introduces bilinear terms and logarithms which cause difficult to solve the model. For example, it is well know that Eq. (26) frequently causes convergence problems for NLP solvers. However, computational difficulties due to Eq. (26) can be avoided by using appropriate lower and upper bounds on all variables used for the calculation. In this sense, the mathematical model also includes constraints to avoid temperature crosses.

Finally, authors conclude that the proposed model formulation together with the solver selected (SBB solver) are adequate, since different initial values were tried and the model always achieved the same optimal solutions. Scaling on variables and equations were taken into account in order to increase the robustness and assure the convergence of the model.

The computational performance of SBB solver was compared with other MINLP solver (DICOPT+) which is also supported by GAMS. DICOPT decomposes the MINLP problem into a series of nonlinear program (NLP) and MILP sub-problems using an outer approximation formulation – Quesada and Grossmann [11]. Both solver performances were compared using the same initial values. From the results, it is concluded that the computational difficulties (nonlinearities/nonconvexities) are dominant compared to the combinatorial (integer) ones because the SBB algorithm resulted more efficient than DICOPT to solve the problem. In fact, SBB converged in all cases in contrast to the DICOPT solver performance. When the convergence problems appeared by using DICOPT, other initial values were adopted but the problems still persisted. From this, it can be concluded that the DICOPT solver is strongly influenced by the initial values rather than SBB solver.

Same qualitative conclusions were reported by Savola et al. [12] for other process system. The authors developed an MINLP model for small-scale combined heat and power (CHP) plant synthesis and operation. In that paper, binary variables are used to select the optimal configuration of system. Also, a sensitive analysis so as to check of the effect of SBB and DICOPT solvers on the model solution showed that SBB solver is more efficient than DICOPT solver despite its "slow" convergence velocity.

6. Conclusions. Future works

A detailed MINLP model for the optimal design of furnaces/fired heaters is developed. The process is modelled by considering detailed energy, mass and momentum balances. Constraints Eqs. (1)–(53) describe the complete steady state model for the fired heater shown in Fig. 1a. Nonlinear correlations to compute physical and chemical properties of air, oil, flue gases, overall radiant exchange factor, convection coefficient, overall heat transfer coefficient among others, have been derived from Wimpress [2] and Couper et al. [10].

The fired heater MINLP model considers discrete decisions (integer variables) tube arrays and number of convection and radiation tubes. The model also involves constraints on geometric design (length, height and width) in order to obtain feasible and realistic designs.

Table 4
Optimal solution for Case Study II. Comparison between Design II and Design I.

Variable	MINLP Design II (minimizing the heat transfer area + refractory area)	MINLP Design I
Nt^{Rad}	76	96
Nt^{Conv}	80	108
Row_{Conv}	20	18
Nt^{Shield}	4	6
Comp	2	3
η_{FH}	0.774	0.774
A (m^2)	403.4157	414.8120
Q_n (MWatt)	28.3868	28.3745
Gas Flux (Kg/s)	12.3263	12.3209
Q_{rad} (MWatt)	14.8455	14.9322
h_c (KJ/Kg)	793.4172	791.4889
T_c (K)	526.2588	525.5788
T_w (K)	633.8711	633.5311
W (m)	4.906	6.096
H (m)	6.5961	7.62
$tube_l$ (m)	15.1784	12.192
E_l (m)	14.7212	11.7348
A_{rad} (m^2)	401.7449	404.5227
A_{cp}^{shield} (m^2)	11.9653	14.307
A_{cp}^{wall} (m^2)	215.3758	214.606
A_R (m^2)	192.9469	202.711
MBL (m)	5.2072	5.445
PL (KPa.m)	122.2383	127.859
T_g (K)	1157.1738	1151.4166
Flux (Watt/m^2)	36,952.7912	36,913.5827
Q_{conv} (MWatt)	7.126	7.039
T_s (K)	700.3172	699.662
LMTD (K)	655.429	653.0877
T_{wc} (K)	551.926	551.586
T_{gc} (K)	896.4283	893.747
T_{gf} (K)	696.4	694.888
G (Kg/m^2s)	1.8309	1.6551
h_{Cc} (Watt/(m^2 K))	27.3294	25.6146
h_{Cr} (Watt/(m^2 K))	12.5659	12.503
h_{Cw} (Watt/(m^2 K))	53.5403	53.443
h_C (Watt/(m^2 K))	45.4942	45.653
U (Watt/(m^2 K))	42.1213	41.7522
A_{conv} (m^2)	422.8895	455.0881
p_h (Pa)	4.4791	3.4837
Δp_f (Pa)	44.044	32.1
V_s (m/s)	8.6868	8.8431
p_{hs} (Pa)	20.156	20.902
Ds (m)	1.8464	1.8288
D_{stack} (Pa)	136.364	118.696
H_s (m above shield tubes)	22.86	19.92
Area (tubing and refractory) (m^2)	1434.516	1482.66
$Nt^{wallside}$	60	72
Nt^{ceil}	12	18
R_{cost} ($/yr)	132,330	133,240
C_{cost} ($/yr)	81,935.002	88,173.51
FB_{cost} ($/yr)	88,886.627	92,274.982
O_{cost} ($/yr)	1,549,800	1,549,100
Total annual cost ($/yr)	1,852,900	1,862,800
Iteration number	310	14
CPU time (s)	0.047	0.063

Table 5
Optimal solution for Case Study III. Comparison between Design III and Design II.

Variables	MINLP Design III (minimizing TAC)	MINLP Design II (minimizing total area)
Nt^{Rad}	76	76
Nt^{Conv}	92	80
Row_{Conv}	23	20
Nt^{Shield}	4	4
Comp	2	2
Nt^{Bank}	18	18
η_{FH}	0.788	0.774
A (m^2)	392.3608	403.4157
Q_n (MWatt)	27.8933	28.3868
Gas flux (Kg/s)	12.111	12.3263
Q_{rad} (MWatt)	14.4926	14.8455
h_c (KJ/Kg)	801.2674	793.4172
T_c (K)	529.0144	526.2588
T_w (K)	635.248	633.8711
W (m)	5.795	4.906
H (m)	5.795	6.5961
$Tube_l$ (m)	14.485	15.1784
E_l (m)	14.028	14.7212
A_{rad} (m^2)	382.8423	401.7449
A_{cp}^{shield} (m^2)	11.4023	11.9653
A_{cp}^{wall} (m^2)	205.242	215.3758
A_R (m^2)	191.7949	192.9469
MBL (m)	5.1873	5.2072
PL (KPa m)	121.77	122.2383
T_g (K)	1163.123	1157.1738
Flux (Watt/m^2)	37,855.0893	36,952.7912
Q_{conv} (MWatt)	7.478	7.126
T_s (K)	673.98	700.3172
LMTD (K)	637.2683	655.429
T_{wc} (K)	553.304	551.926
T_{gc} (K)	879.645	896.4283
T_{gf} (K)	688.6966	696.4
G (Kg/m^2s)	1.8894	1.8309
h_{Cc} (Watt/(m^2 K))	27.766	27.3294
h_{Cr} (Watt/(m^2 K))	12.259	12.5659
h_{Cw} (Watt/(m^2 K))	53.9435	53.5403
h_C (Watt/(m^2 K))	45.6532	45.4942
U (Watt/(m^2 K))	42.2576	42.1213
A_{conv} (m^2)	463.44	422.8895
p_h (Pa)	4.4791	4.4791
Δp_f (Pa)	52.754	44.044
V_s (m/s)	8.791	8.6868
p_{hs} (Pa)	21.4	20.156
Ds (m)	1.78	1.8464
D_{stack} (Pa)	156.52	136.364
H_s (m above shield tubes)	27.215	22.86
Area (tubing and refractory) (m^2)	1468.602	1434.516
$Nt^{wallside}$	52	60
Nt^{ceil}	20	12
R_{cost} ($/yr)	126,100	132,330
C_{cost} ($/yr)	89,791.828	81,935.002
F_{cost} ($/yr)	90,983.843	88,886.627
O_{cost} ($/yr)	1,522,800	1,549,800
Total annual cost ($/yr)	1,829,700	1,852,900
Iteration number	163	310
CPU time (s)	0.047	0.047

The model proved to be robust and flexible. Different case studies considering various objective functions are successfully solved without convergence difficulties. Results here obtained are summarized in Table 6. MINLP-Design I agree satisfactorily with the one reported in [2], while the optimal MINLP-Design II and optimal economic MINLP-Design III reflect a substantial improvement in their operative and economic performance as well as in their designs, according to the objective function optimized.

Global optimal solutions can not be guaranteed due to the non-convex constraints involved in the mathematical model.

Large nonlinear optimization problems are characterized by convergence problems (infeasible solutions) and local optimal solutions. Scaling on variables and equations as well as a systematic initialization procedure are implemented in order to guarantee the model convergence.

As future works, the developed model will be extended in order to optimize simultaneously the configuration and operating conditions as well. For this, a superstructure embedding alternative designs for fired heaters and/or furnaces will be developed. For example, binary variables (0–1) should be introduced in order to select the optimal tube arrangement, number of burners and their

Table 6
Optimal values obtained for the main variables.

Variable	MINLP Design I	MINLP Design II	MINLP Design III
Fired heater volume (m^3)	594.164	523.834	523.016
Total height (m)	27.547	29.456	33.011
Total heat transfer area (m^2)	893.102	850.245	873.86
Total refractory area (m^2)	574.058	570.81	581.91
Investment capital ($/yr)	1,742,713.84	1,684,175.72	1,704,864.84
Operating cost ($/yr)	1,549,100	1,549,800	1,522,800
Total annual cost ($/yr)	1,862,800	1,852,900	1,829,700
η_{FH}	0.774	0.774	0.788

allocations. Therefore, the resulting mathematical model will be used not only to optimize the operating conditions but also its configuration.

On the other hand, the presented mathematical model will be complemented by other models developed previously by some of the authors; for example models for synthesis and design of Dual Purpose Desalination Plants (DPDPs) in which gas turbines and steam turbines (back-pressure, extraction-condensing turbines) are considered for electricity production while thermal desalination processes are considered for fresh-water production. Then, it would be attractive to extend the proposed superstructures in order to embed other alternatives for steam generation.

Finally, it is interesting to explore "hybrid methodologies" for the optimal design of fired heaters by combining the advantages of MINLP and CFD techniques. For example, one strategy could be based on the following idea. Firstly the MINLP model is solved in order to obtain the optimal configuration and operating conditions and then in a second phase, a CFD model is applied to the obtained configuration. The CDF model is solved by using the MINLPs detailed solution (temperature, pressure profiles and other critical variables) as starting point for the CFD solution algorithm.

So, complete and detailed designs for heat transfer equipments can be achieved. Moreover, the proposed methodology could be extended to other process equipments.

Acknowledgements

Financial supports obtained from the Consejo Nacional de Investigaciones Científicas y Técnicas (CONICET), the Agencia Nacional para la Promoción de la Ciencia y la Tecnología (ANPCyT), the Universidad Tecnológica Nacional Facultad Regional Rosario (UTN-FRRo)-Argentina are greatly acknowledged. Fruitful discussions with Mr. Jorge Arroyo are also greatly appreciated.

Finally, a special thanks to the reviewers who have provided quite valuable comments on the presented work.

References

[1] A. Brooke, D. Kendrick, A. Meeraus, A. A. GAMS – A User's Guide (Release 2.25), The Scientific Press, San Francisco, CA, 1992.
[2] R.N. Wimpress, Rating fired heaters, Hydrocarbon Processing & Petroleum Refiner 42 (10) (1963) 115–126.
[3] P. Stehlík, J. Kohoutek, V. Jebácek, Simple mathematical model of furnaces and its possible applications, Computers and Chemical Engineering 20 (11) (1996) 1369–1372.
[4] Z. Jegla, P. Stehlík, J. Kohoutek, Plant energy saving through efficient retrofit of furnaces, Applied Thermal Engineering 20 (15–16) (2000) 1545–1560.
[5] Z. Jegla, The conceptual design of a radiant chamber and preliminary optimization of a process tubular furnace, Heat Transfer Engineering 27 (6) (2006) 50–57.
[6] Marek Sarlej, Pavel Petr, Jirı Hajek, Petr Stehlik, Computational support in experimental burner design optimisation, Applied Thermal Engineering 27 (16) (2007) 2727–2731.
[7] M. Miltner, A. Miltner, M. Harasek, A. Friedl, Process simulation and CFD calculations for the development of an innovative baled biomass-fired combustion chamber, Applied Thermal Engineering 27 (7) (2007) 1138–1143.
[8] Q. Guimarães, C. Fontes da Costa e Silva, Process optimization through computational fluid dynamics. Case studies, in: 2nd Mercosur Congress on Chemical Engineering 4th Mercosur Congress on Process Systems Engineering, (ENPROMER-2005), Village Rio das Pedras, Club Med, Rio de Janeiro, Brazil, Agosto, 2005.
[9] W.E. Lobo, J.E. Evans, Heat transfer in the radiant section of petroleum heaters, Trans AIChE 35 (1939) 743–778.
[10] J.R. Couper, W.R. Penney, J.R. Fair, M. Stanley, M. Walas, Chemical Process Equipment Selection and Design, Copyright, Gulf Professional Publishing, Elsevier, 2005.
[11] I.E. Quesada, I.E. Grossmann, Na LP/NLP based branch and bound algorithm for convex MINLP optimization problems, Computers and Chemical Engineering 16 (1992) 937–947.
[12] T. Savola, T.M. Tveit, C.J. Fogelholm, A MINLP model including the pressure levels and multiperiods for CHP process optimisation, Applied Thermal Engineering 27 (2007) 1857–1867.